JOURNAL OF THEORETICAL
AND APPLIED MECHANICS
48, 1, pp. 27-44, Warsaw 2010

MODEL OF GASODYNAMIC CONTROL SYSTEM FOR GUIDED BOMBS

Robert Głębocki
Marcin Żugaj

Warsaw University of Technology, Institute of Aeronautics and Applied Mechanics, Warsaw, Poland
e-mail: rgleb@meil.pw.edu.pl, zugaj@meil.pw.edu.pl

In this paper, a new concept of the control system for guided bombs is described. Authors propose a gasodynamic method for the air bomb control. In the presented method, the bomb control is realised by a set of single-use impulse control engines. The gasodynamic controlled bomb dynamic and aerodynamic models are described. Some results of numerical simulations are presented as well.

Key words: guided bombs, flight control system

Notationa

$\mathbf{A}$	–	inertia matrix
$\mathbf{B}$	–	gyroscopic matrix
C_X, C_Y, C_Z	–	coefficients of aerodynamic force
C_R, C_M, C_N	–	coefficients of aerodynamic moments
$\boldsymbol{f}_a, \boldsymbol{f}_A$	–	vector of aerodynamics force and loads, respectively
$\boldsymbol{f}_g, \boldsymbol{f}_G$	–	vector of gravity force and loads, respectively
$\boldsymbol{f}_{si}$	–	vector of i-th impulse engine force
$\boldsymbol{f}_S$	–	vector of control loads
g	–	gravity acceleration
I_x, I_y, I_z	–	moments of inertia of bomb
k_S	–	control signal activates the impulse engine
l, m	–	bomb length and mass, respectively
$\boldsymbol{m}_a, \boldsymbol{m}_g, \boldsymbol{m}_{si}$	–	vector of aerodynamic, gravity and i-th impulse engine moment, respectively
n_S	–	active engine number
P, Q, R	–	angular velocities, components of state vector $\boldsymbol{x}$
P_{Si}	–	i-th engine thrust value

$\boldsymbol{r}_c$	–	centre of gravity position vector
S	–	maximum area of the bomb body cross-section in $0yz$ plane
S_x	–	bomb static mass moments
$\boldsymbol{T}_V, \boldsymbol{T}_\Omega$	–	velocity and angle transformation vector, respectively
U, V, W	–	linear velocities, components of state vector $\boldsymbol{x}$
$\boldsymbol{v}$	–	vector of linear velocity
$\boldsymbol{x}$	–	state vector
x_c	–	centre of gravity coordinates in x axis, component of centre of gravity vector position $\boldsymbol{r}_c$
x_1, y_1, z_1	–	bomb position coordinates, components of position and attitude vector $\boldsymbol{y}$
$\boldsymbol{y}$	–	position and attitude vector
ϕ, θ, ψ	–	bomb euler angles, components of the position and attitude vector $\boldsymbol{y}$
γ_{Si}	–	angle of i-th engine position
ρ	–	air density
$\boldsymbol{\Omega}$	–	velocities and rates matrix

1. Introduction

The contemporary development of air-launched weapons is mostly oriented on design of precision-guided munitions. The percentage of guided weapons in all instruments of war used from air is greater in each subsequent military conflict. For example, at the operation Desert Storm 18 percent of used by US Army bombs were controlled, at the operation Iraq Freedom the same factor was about 66 percent. In the last ten years this development was closely connected with Global Positioning System and Inertial Navigation System. Especially, since GPS has reached full availability, many navigation systems of guided missiles and bombs are based on INS/GPS. Well known is Joint Direct Attack Monition, which was widely used during operations in Kosovo, Afghanistan and Iraq. There are also other constructions like AASM carried out by SAGEM and SPICE carried out by RAFAEL (Fig. 1). All these bombs are aerodynamically controlled.

One of the possibilities of development of guided bombs is taking advantage of new concepts for control of the object. In the present control systems, the bomb is controlled with small single-use rocket engines with thrust directed normally to the main axis of symmetry of the object.

AASM

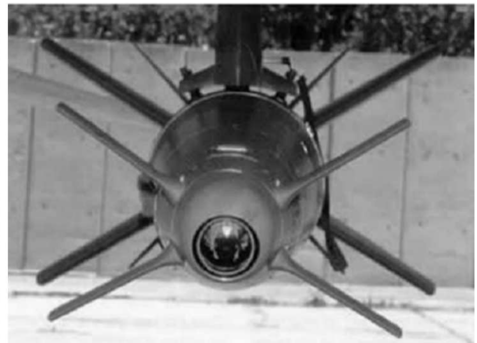

SPICE

Fig. 1. Bombs AASM and SPICE

2. Problem description

In this paper, a new concept of the control system for guided bombs is described. The gasodynamic steering kit is proposed instead of aerodynamic one. The bomb is controlled by a set of impulse correction engines. The engines are mounted around the bomb (Fig. 4). The correcting impulses from rocket engines are perpendicular to the main symmetry axis of the flying object and influence directly the centre of gravity of the guided bomb. The impulse rocket engines, used only one time each, correct the trajectory. The presented solution of the control system with impulse correction engines needs slow spin of the bomb. The bomb aft section is fitted with fins to give the bomb aerodynamic stability and spin. The fins are immediately unfolded after the bomb drop and their fixed cant angle gives the object a slow spin (about 20-30 rad/s). The rotation velocity of the bomb depends on the velocity of flight. The much less range than in the case of aerodynamic control objects require that bombs have to be accurately launched over the target operating area. The control process starts when the pitch angle is higher than 45%. The earlier control system is ineffective. In the next stage of flight, the object is automatically guided to the target.

The system is based on a set of single-use impulse engines. It can correct the flight trajectory only about 700 m from the uncontrolled one. But the control system hardware is very simple. There are not movable devices on the bomb board. It makes them the potential to be cheaper and more reliable than systems with aerodynamic control. A similar gasodynamic control system is successfully used in guided mortar missiles like STRIX carried out by SAAB and BOFORS. The bomb can be dropped from altitude of about four to ten thousand meters using this control system, and the whole fall takes about twenty to thirty seconds. In this concept, guided bombs do not have as long range as JDAM (Joint Direct Attack Munition) but are potentially cheaper and have less complicated hardware. They can be used for precision bombing at the battlefield.

2.1. Dynamics of impulse control of flying objects

Classic methods of control of a flying object make assumptions that:

- steering forces initially change the moment acting on the object, then this moment rotates the object around its gravity centre;
- supporting surfaces get necessary angles of attack and produce steering forces.

This way, the object is turned at first around the mass centre, then this movement effects on the mass centre velocity vector. This solution is characterized by inertia and a "long" time gap between control system decisions and execution of its commands. This effect delays the control. This fault can be limited by the direct action on motion of the gravity centre. In the presented method, the control of the missile is performed by the set of correction rocket engines. These engines act on the gravity centre of the object (Fig. 2).

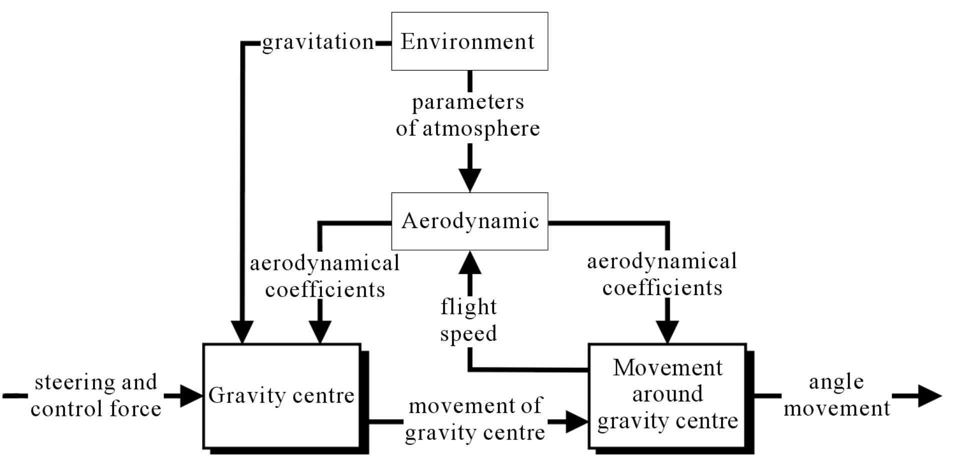

Fig. 2. Block scheme of the object dynamics

In this method of the flying object control we make assumptions that:

- steering forces influence first the object gravity centre;
- rotation around the gravity centre is an effect of gravity centre translation and aerodynamic interaction.

Solution of this kind gives more effective influence on the speed vector. A block scheme of the object dynamics is shown in Fig. 2.

2.2. Missile guidance system

In the spinning object, one channel is used to control the object in both horizontal and vertical planes. This can be realised by a gasodynamic impulse acting on the object gravity centre. The method was described in more details in papers by Głębocki and Vogt (2007) and Głębocki and Żugaj (2009). This solution can precisely guide the object to the attacked target. It also makes the operation of the servo-control system easier. Complicated structure of the aerodynamic servo is not needed, either. Also the board power demand for the gasodynamic system is much less than in the aerodynamic one. Electric energy supplies only electronic devices, not control surfaces. It makes the equipment on the missile board smaller and easier to made, but it complicates the guidance logic and dynamics of the object controlled flight.

As was said earlier, in the presented concept the control is realised by correction engines located around the flying object centre of gravity. In our simulations we tested different numbers of correction engines from 12 to 20. The tracking technique made it possible to introduce several course corrections in a rapid succession. If necessary, all rocket correction engines can be used for the control process in the last few seconds of the flight.

The task of the rocket engines is to correct the course of the bomb in the second stage of flight, when the pitch angle is over $45°$. The control system homing it to the target, enables the object to achieve a direct hit. The correction rocket engines are located in a cylindrical unit, arranged radially around the periphery. Each correction rocket engine can be fired individually only once in a selected radial direction.

The correction engine set is placed close to the centre of gravity of the projectile. When the rocket engine is fired, the course of the missile is changed instantaneously. By successive firing of several rocket engines, the object is steered with high precision onto the target. The chosen steering system gives a very fast response to the guidance signals.

The decision when the correcting rocket engine should be fired depends on the value of the control error and its derivative. The frequency of firing of the correcting engines N is defined as the number of rotations of the mortar missile between the correcting engines firing. N increases with the control signal value K. The direction of control forces depends on the time of firing of the control engine. The time of control engines firing depends on the target direction, position of the correction engine, roll angle and angular velocity ω_x along the axis $\boldsymbol{x}$.

The time of correction engine work t_k should be as short as possible. Tests have shown that this time should not be longer than $1/4$ time of the bomb turn. During this time, the impulse of the correction engine changes the bomb course, which leads the object main symmetry axis.

A single-channel direct discontinuous impulse control method imposes requirements on control quality for the optimal correction engines firing algorithm and good dynamic stability of the bomb (Iglesian and Urban, 2000). This control method, in contrast to the aerodynamic control, does not require any compromise between stability and controllability, because the stability value of the bomb does not have the upper limit. Stability has to be much higher than in the case of aerodynamic control. However, this method makes algorithms of correction engines firing more complicated. The sequence of firing should be such that the unbalance of the bomb is minimal. This algorithm should give the value of the mean effect of control proportional to the control signal value.

3. Nonlinear simulation model of guided bomb

3.1. Dynamics model

In the simulation, the bomb is modelled as a rigid body with six degrees of freedom. In this case, the control force is produced by a set of impulse engines placed around the bomb centre of gravity. The bomb rotates around its axis of symmetry during the fall. Each engine is activated separately in appropriate angle of the bomb turn and works in a short period of time. The vector of the engine force is perpendicular to the axis of bomb symmetry and displaces the bomb centre of gravity.

Equations of motion of the bomb are derived in the co-ordinate system $0xyz$, Fig. 3 (Maryniak, 1978) fixed to the bomb body. The centre 0 of the system is placed at an arbitrary point in the bomb axis of symmetry. The $0x$ axis lies in the axis of bomb symmetry and is directed forward. The $0y$ axis is perpendicular to the axis of bomb symmetry and points right, the $0z$ axis points "down".

The bomb translations and attitude angles are calculated in the inertial co-ordinate system $0_1x_1y_1z_1$; the centre of this system 0_1 is placed at an arbitrary point on the earth surface. The 0_1z_1 axis is placed along the vector of gravity acceleration and points down. The $0_1x_1z_1$ plane is horizontal, tangent to the earth surface, the 0_1x_1 axis points to the North, and 0_1y_1 axis to the East.

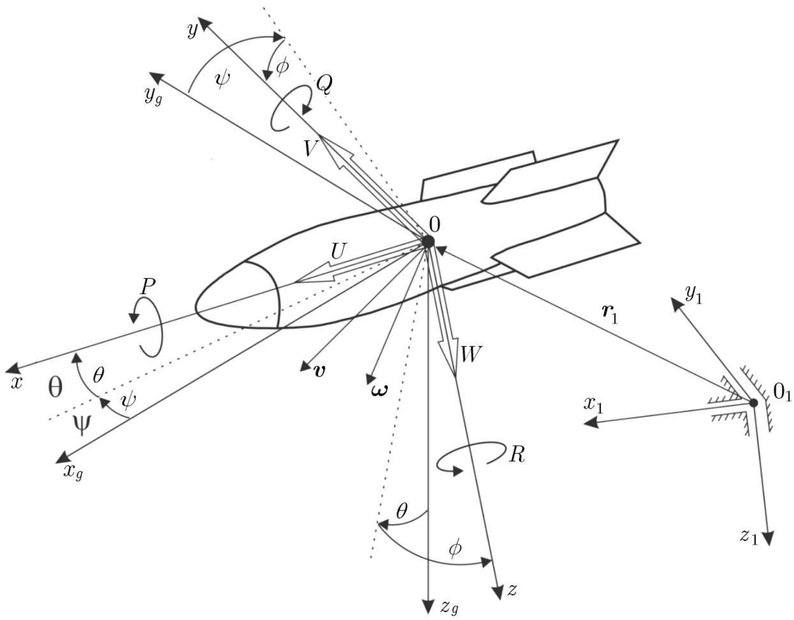

Fig. 3. Co-ordinate systems

A relationship between the bomb state vector $\boldsymbol{x} = [U, V, W, P, Q, R]^\top$ and the vector describing position and attitude $\boldsymbol{y} = [x_1, y_1, z_1, \phi, \theta, \psi]^\top$ is given by

$$\dot{\boldsymbol{y}} = \mathbf{T}\boldsymbol{x} \tag{3.1}$$

The matrix $\mathbf{T}$ has form

$$\mathbf{T} = \begin{bmatrix} \mathbf{T}_V & \mathbf{0} \\ \mathbf{0} & \mathbf{T}_\Omega \end{bmatrix} \tag{3.2}$$

where the velocity transformation matrix $\mathbf{T}_V$ is

$$\mathbf{T}_V = \begin{bmatrix} \cos\theta\cos\psi & \sin\theta\sin\phi\cos\psi - \cos\phi\sin\psi & \cos\phi\sin\theta\cos\psi + \sin\phi\sin\psi \\ \cos\theta\sin\psi & \sin\theta\sin\phi\sin\psi + \cos\phi\cos\psi & \cos\phi\sin\theta\sin\psi - \sin\phi\cos\psi \\ -\sin\theta & \sin\phi\cos\theta & \cos\phi\cos\theta \end{bmatrix} \tag{3.3}$$

and the transformation matrix for the angles $\mathbf{T}_\Omega$ is

$$\mathbf{T}_\Omega = \begin{bmatrix} 1 & \sin\phi\tan\theta & \cos\phi\tan\theta \\ 0 & \cos\phi & -\sin\phi \\ 0 & \sin\phi\sec\theta & \cos\phi\sec\theta \end{bmatrix} \tag{3.4}$$

The roll angle ϕ, the pitch angle θ and the azimuth angle ψ describe the attitude of the bomb (Fig. 4) and the components of the vector $\boldsymbol{r}_1 = [x_1, y_1, z_1]$ describe the bomb position in the $0x_1y_1z_1$ system of co-ordinates.

The bomb equations are obtained by summing up the inertia (left hand side of the equation), gravity $\boldsymbol{f}_G$, aerodynamic $\boldsymbol{f}_A$ and control $\boldsymbol{f}_S$ loads (forces and moments) acting on the bomb (Maryniak, 1978)

$$\mathbf{A}\dot{\boldsymbol{x}} + \mathbf{B}(\boldsymbol{x})\boldsymbol{x} = \boldsymbol{f}_A(\boldsymbol{x}, \boldsymbol{y}) + \boldsymbol{f}_G(\boldsymbol{y}) + \boldsymbol{f}_S(\boldsymbol{y}, k_S, n_S) \tag{3.5}$$

where k_S is the control signal activating the impulse engine and n_S is the number of the active engine.

The left-hand side of equation (3.5) describes the inertia loads in the bomb frame of reference. The inertia matrix $\mathbf{A}$ has form

$$\mathbf{A} = \begin{bmatrix} m & 0 & 0 & 0 & 0 & 0 \\ 0 & m & 0 & 0 & 0 & S_x \\ 0 & 0 & m & 0 & -S_x & 0 \\ 0 & 0 & 0 & I_x & 0 & 0 \\ 0 & 0 & -S_x & 0 & I_y & 0 \\ 0 & S_x & 0 & 0 & 0 & I_z \end{bmatrix} \tag{3.6}$$

where: m is the bomb mass, S_x is the bomb static mass moments and I_x, I_y, I_z are the bomb moments of inertia.

The gyroscopic matrix $\mathbf{B}(\boldsymbol{x})$ is calculated as

$$\mathbf{B}(\boldsymbol{x}) = \boldsymbol{\Omega}(\boldsymbol{x})\mathbf{A} \tag{3.7}$$

where the matrix of velocities and rates $\boldsymbol{\Omega}(\boldsymbol{x})$ has form

$$\boldsymbol{\Omega}(\boldsymbol{x}) = \begin{bmatrix} 0 & -R & Q & 0 & 0 & 0 \\ R & 0 & -P & 0 & 0 & 0 \\ -Q & P & 0 & 0 & 0 & 0 \\ 0 & -W & V & 0 & -R & Q \\ W & 0 & -U & R & 0 & -P \\ -V & U & 0 & -Q & P & 0 \end{bmatrix} \tag{3.8}$$

The vector of gravity force acting on the body is calculated as

$$\boldsymbol{f}_g(\boldsymbol{y}) = mg \begin{bmatrix} -\sin\theta \\ \cos\theta\sin\phi \\ \cos\theta\cos\phi \end{bmatrix} \tag{3.9}$$

where g is the gravity acceleration.

The point 0 is placed at the bomb centre of gravity, the vector of moment from gravity forces is

$$\boldsymbol{m}_g(\boldsymbol{y}) = \boldsymbol{r}_c \times \boldsymbol{f}_g(\boldsymbol{y}) \tag{3.10}$$

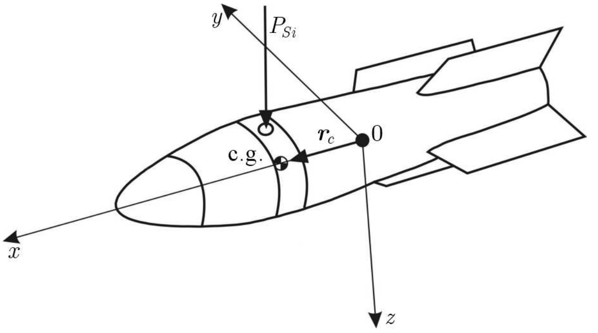

Fig. 4. Set of impulse engines

where $\boldsymbol{r}_c = [x_c, 0, 0]^\top$ is the vector of centre of gravity position in the bomb system of coordinates (Fig. 4).

Combining (3.9) and (3.10), the vector of gravity loads acting on the bomb is calculated as

$$\boldsymbol{f}_G(\boldsymbol{y}) = \begin{bmatrix} \boldsymbol{f}_g(\boldsymbol{y}) \\ \boldsymbol{m}_g(\boldsymbol{y}) \end{bmatrix} \tag{3.11}$$

The bomb has a set of impulse engines placed at the bomb body around the centre of gravity (Fig. 4). The vector of i-th impulse engine force has form

$$\boldsymbol{f}_{Si}(\boldsymbol{y}, k_S, n_S) = P_{Si} k_S \begin{bmatrix} 0 \\ -\cos\gamma_{Si} \\ \sin\gamma_{Si} \end{bmatrix} \tag{3.12}$$

where P_{Si} is the value of engine thrust, γ_{Si} is the angle of engine position (Fig. 5).

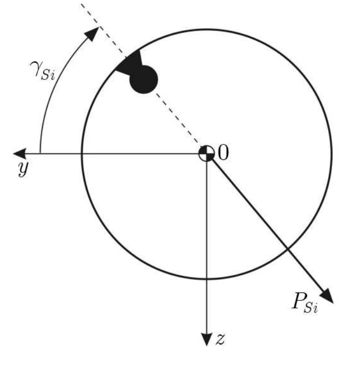

Fig. 5. Position of the impulse engine

The number of engine n_S gives information about the thrust and angle position of the given engine. The control signal k_S is used to activate the engine and is calculated using the control error and actual bomb attitude. It can have value 0 or 1.

The vector of moment from the impulse engine forces of each engine is equal

$$\boldsymbol{m}_{Si}(\boldsymbol{y}) = \boldsymbol{r}_c \times \boldsymbol{f}_{Si}(\boldsymbol{y}, k_S, n_S) \tag{3.13}$$

The vector of impulse engines forces acting on the bomb is calculated from (3.12) and (3.13) as

$$\boldsymbol{f}_S(\boldsymbol{y}, k_S, n_S) = \begin{bmatrix} \boldsymbol{f}_{Si}(\boldsymbol{y}, k_S, n_S) \\ \boldsymbol{m}_{Si}(\boldsymbol{y}) \end{bmatrix} \tag{3.14}$$

The bomb aerodynamic loads are calculated using coefficients describing the loads acting on the whole bomb. The force and moment vectors are calculated as

$$\boldsymbol{f}_a(\boldsymbol{x}, \boldsymbol{y}) = \frac{1}{2}\rho(z_1)|\boldsymbol{v}|^2 S \begin{bmatrix} C_X(\boldsymbol{x}) \\ C_Y(\boldsymbol{x}) \\ C_Z(\boldsymbol{x}) \end{bmatrix} \qquad \boldsymbol{m}_a(\boldsymbol{x}, \boldsymbol{y}) = \frac{1}{2}\rho(z_1)|\boldsymbol{v}|^2 Sl \begin{bmatrix} C_R(\boldsymbol{x}) \\ C_M(\boldsymbol{x}) \\ C_N(\boldsymbol{x}) \end{bmatrix} \tag{3.15}$$

where: S is the maximum area of the bomb body cross-section in $0yz$ plane (Fig. 4), l – bomb length, $\rho(z_1)$ – air density, $\boldsymbol{v}$ – vector of linear velocity and C_X, C_Y, C_Z, C_R, C_M, C_N are force and moment coefficients.

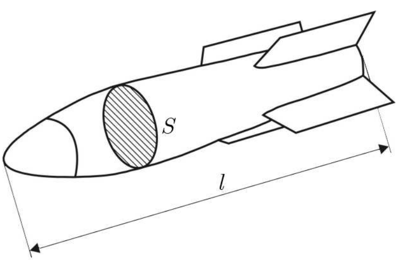

Fig. 6. Aerodynamic parameters of the bomb

The aerodynamic loads in the equations of motion are calculated as

$$\boldsymbol{f}_A(\boldsymbol{x}, \boldsymbol{y}) = \begin{bmatrix} \boldsymbol{f}_a(\boldsymbol{x}, \boldsymbol{y}) \\ \boldsymbol{m}_a(\boldsymbol{x}, \boldsymbol{y}) \end{bmatrix} \tag{3.16}$$

The bomb stabilizers generate the aerodynamic moment along the x axis. The moment value depends on the angle of incidence, area, shape and position of stabilizers, bomb air speed, angle of attack and angle of sideslip.

The equations of bomb motion are combined with the model of the control system. The control system calculates the control signal and selects the proper impulse engine.

3.2. Aerodynamical model

The Computational Fluid Dynamics (CFD) method was used to obtain the aerodynamic coefficients. The bomb has a cylindrical shape and aerodynamic phenomena in the $0xy$ plane of symmetry are similar as in the $0xy$ plane of symmetry. So, it was assumed that the aerodynamic load can be calculated as a sum of lateral $(0xy)$ and longitudinal $(0xz)$ loads. The non-rotating bomb was considered in this calculation.

The coefficients were derived in the aerodynamical coordinate system $0_A x_A y_A z_A$ (Fig. 7) fixed to the bomb tip. The $0_A x_A$ axis lies in the axis of bomb symmetry and is directed backwards. The $0_A y_A$ axis is perpendicular to the axis of bomb symmetry and points right, and the $0_A z_A$ axis points up.

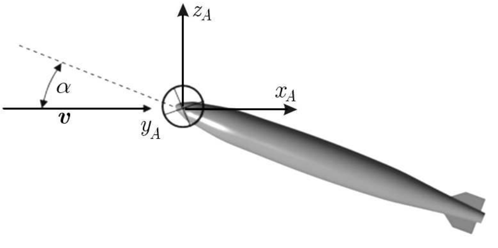

Fig. 7. Aerodynamical co-ordinate system of the bomb

The lift CL, drag CD and aerodynamic moment Cm coefficients were calculated for the Mach number 0.56 and 1.16. Next, the aerodynamic centre was obtained and aerodynamic coefficients were transformed to this point. The aerodynamic moment at aerodynamic centre is denoted as Cm_{ac} (Fig. 8).

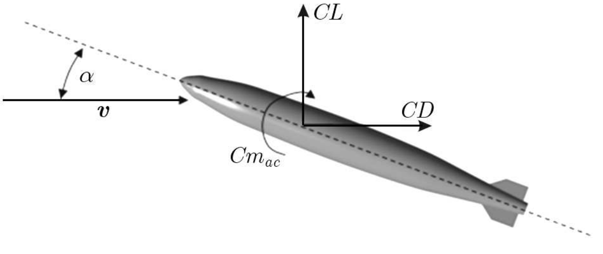

Fig. 8. Aerodynamical coefficients of the bomb

The aerodynamic centre is placed at 26.67% and 30% of the bomb length for Ma = 0.56 and 1.16, respectively. The coefficients as function of the angle of attack are shown in Figs. 9 to 11.

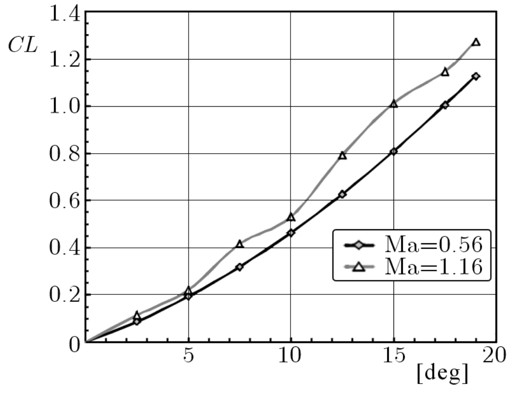

Fig. 9. Lift coefficient

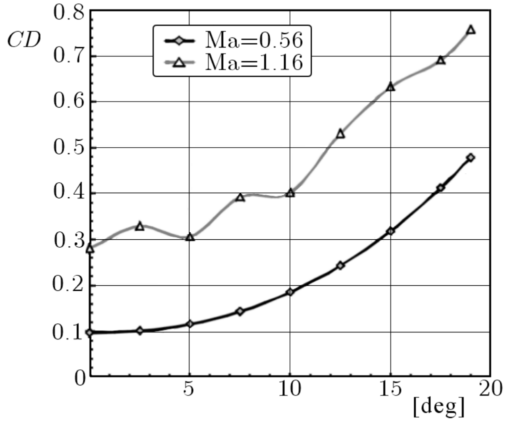

Fig. 10. Drag coefficient

The pitch dynamic derivative dCM, which is given in the body fixed coordinate system $0xyz$, was obtained as well. The derivative changes versus the angle of attack as shown in Fig. 12.

The force and moment coefficients C_X, C_Y, C_Z, C_R, C'_M, C'_N are obtained by transformation of the CL, CD and Cm_{ac} coefficients to the body fixed coordinate system $0xyz$ for lateral $(0xy)$ and longitudinal $(0xz)$ motion separately. The whole pitch and yaw moments are calculated using equations

$$C_M = C'_M + dCM \cdot Q \qquad\qquad C_N = C'_N + dCM \cdot R \tag{3.17}$$

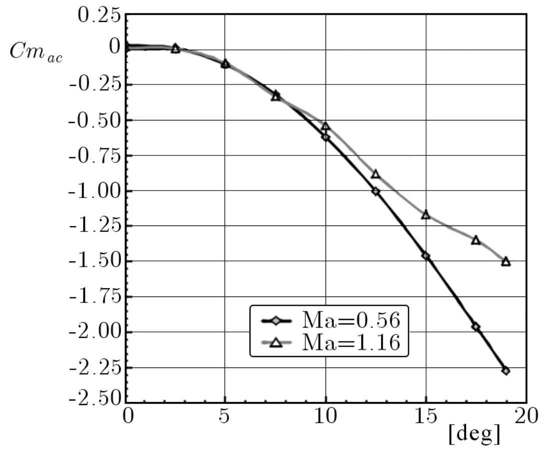

Fig. 11. Moment coefficient

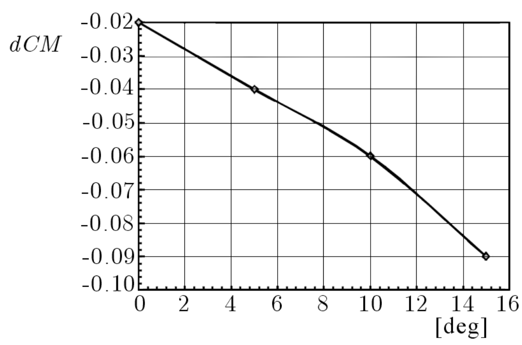

Fig. 12. Pitch derivative coefficient

4. Results

Simulation experiments tested dynamic properties of gasodynamic-controlled bombs. The tests were based on the mathematical model described in Section 4. For simulation experiments, a Matlab/Simulink model was used. Simulations were made for bombs with the following parameters: mass 100 kg, length 1.5 m, and diameter 0.18 m. The bombs were tested with three different rotation coefficients $k_\omega = 5.8$, 12.3, 37 and were dropped from altitudes $H = 1000$, 2000, 4000 m with the initial speed $v = 222$ m/s. Figures 13 and 14 show the us influence of the bombs rotation velocity on their flight. As a result of bomb rotation, we can observe changes in flight trajectories. The gyroscopic effect gets out the trajectory. Figure 13 shows this gyroscopic effect on flight

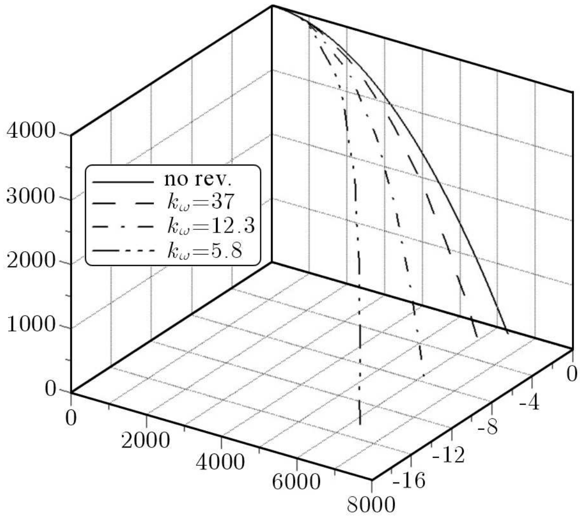

Fig. 13. Gyroscopic effect influencing flight trajectories for different coefficients k_ω

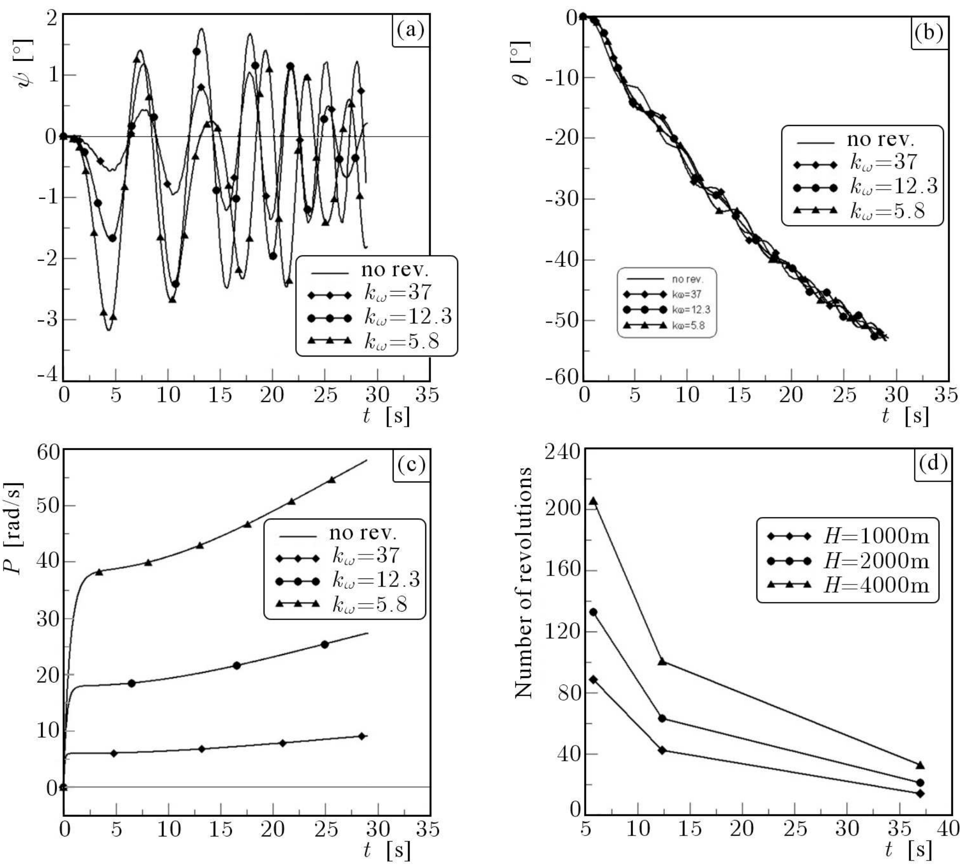

Fig. 14.

trajectories for different coefficients k_ω. In the case when k_ω is equal 5.8, the change of the flight trajectory is above 15 m.

Except for the changes at the flight trajectories, the rotation of the bomb makes small disturbances to the yaw angle (Fig. 14a). The pitch angle disturbances appear in both cases of rotating and non-rotating bombs (Fig. 14b). They come from the low stability margin of the bomb.

Figure 14c describes changes of the spin velocity of bombs during flight. Figure 14d depicts relations between the number of revolutions and flight times (depending on the drop altitude) and coefficients k_ω. These characteristics were used to design the bomb control system.

In Fig. 15, the flight trajectory of a bomb with mass 100 kg dropped from 4000 m with the initial speed $v = 180$ m/s is shown. The bomb has 20 rocket control engines with thrust $P = 10$ kN and the work time $t_k = 0.05$ s. The spin velocity ω_x is about 30 rad/s. Figure 15 gives comparison trajectories for guided and ballistic flight. The bomb can reach the target with error less than 10 m within the range of about 700 m from the uncontrolled fall point. Figure 16 presents time changes of the pitch angle θ during the control flight. We can see that the control process started since about 15 second. It means that first 1000 m in the z_g axis is the ballistic stage of the flight.

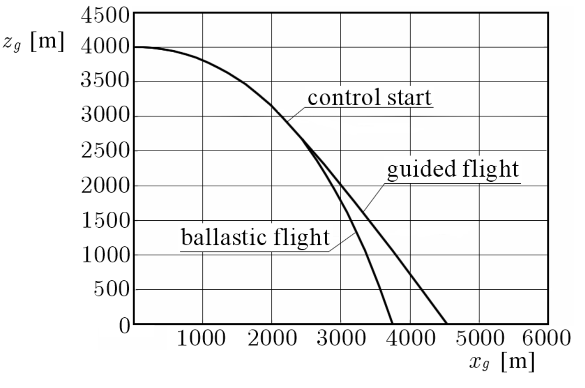

Fig. 15. Controlled and ballistic flight trajectory. The control is realised by 20 correction engines

Figure 17 shows the flight trajectory for a bomb with 12 rocket control engines. The other flight condition were similar as in the case in Fig. 15: mass 100 kg, drop from 4000 m, initial speed $V = 180$ m/s, engine thrust $P = 10$ kN, engine work time $t_k = 0.05$ s, spin velocity ω_x about 30 rad/s. Figure 17 reveals comparison trajectories for the guided and ballistic flight. The bomb can reach the target with error less than 10 m within the range of about 400 m from the uncontrolled fall point. Figure 18 presents time changes of the pitch

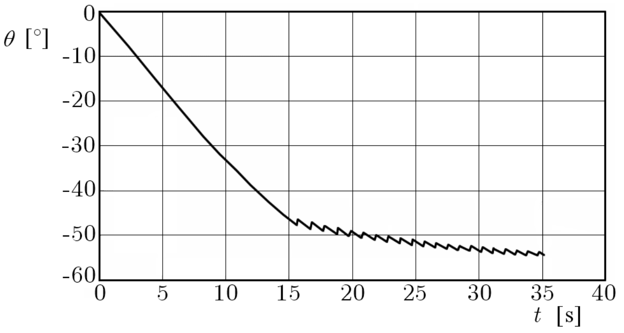

Fig. 16. Pitch angle during the controlled flight. The control is realised by 20 correction engines

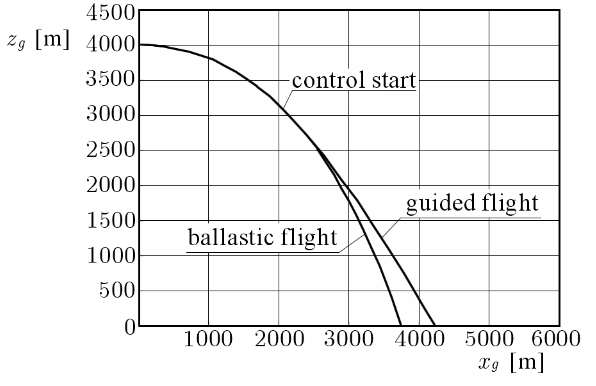

Fig. 17. Controlled and ballistic flight trajectory. The control is realised by 12 correction engines

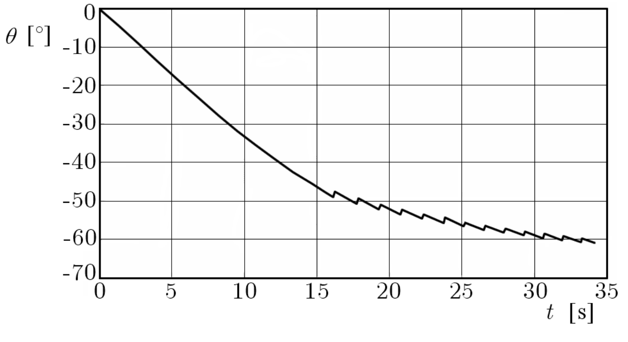

Fig. 18. Pitch angle during the controlled flight. The control is realised by 12 correction engines

angle θ during the controlled flight. Similarly as in Fig. 16, the control process started since about 15 seconds. It means that first 1000 m in the z_g axis was the ballistic stage of the flight.

5. Conclusion

Numerical experiments have shown large possibilities of the objects control by influencing motion of their gravity centre. It is possible to use impulse correction rockets to control falling objects like bombs. This method of control leads to more complicated control algorithms but makes the servo-control easier to operate. The servo has only a correction rocket engines set and the electrical system of initiation.

The presented model and its properties are based on design of a gasodynamic bomb control system with GPS/INS navigation.

Acknowledgment

This work has been supported by Polish Ministry of Science and Higher Education (No. N514-O/0028/32).

References

1. CHEN W.H., 2003, Nonlinear disturbance observer-enhanced dynamic inversion control of missiles, *Journal of Guidance, Control, and Dynamics*, **26**, 1, 161-166
2. ETKIN B., REID D., 1996, *Dynamics of Flight Stability and Control*, 3rd Ed., Wiley, New York
3. GŁĘBOCKI R., VOGT R., 2007, Guidance system of smart mortar missile, *The Archive of Mechanical Engineering*, **LIV**, 1, 47-63
4. GŁĘBOCKI R., ŻUGAJ M., 2009, Gasodynamic control system for INS guided air bombs, *Aerospace Sciences Conference and Exhibit AIAA*, Orlando
5. IGLESIAN P.A., URBAN T.J., 2000, Loop shaping design for missile autopilot, *Journal of Guidance, Control, and Dynamics*, **23**, 3, 516-525
6. KLOTZ H., DERBAK C., 1998, GPS-aided navigation and unaided navigation on the Joint Direct Attack Munition, *IEEE*
7. MARYNIAK J., 1978, Dynamiczna teoria obiektów ruchomych, *Prace Naukowe Politechniki Warszawskiej, Mechanika*, **32**, Wydawnictwo Politechniki Warszawskiej, Warszawa

Model gazodynamicznego systemu naprowadzania lotniczych bomb sterowanych

Streszczenie

W publikacji autorzy przedstawili nowatorski system naprowadzania sterowanych bomb lotniczych. W prezentowanej metodzie układ wykonawczy sterowania oparty jest na zestawie jednorazowych impulsowych silników korekcyjnych oddziałujących bezpośrednio na środek ciężkości sterowanego obiektu. W artykule autorzy zaprezentowali modele dynamiki oraz aerodynamiki bomby sterowanej gazodynamicznie. Oprócz opisu modelu zawarto również wyniki obliczeń aerodynamicznych. Przedstawiono opis systemu sterowania oraz wyniki przeprowadzonych badań symulacyjnych.

Manuscript received March 18, 2009; accepted for print April 15, 2009